Intermediate-velocity atomic collisions. III. Electron capture in 8.6- MeV/amu Ca ions

E. C. Montenegro,* Xiang-Yuan Xu,† W. E. Meyerhof, R. Anholt,‡ and K. Danzmann
Department of Physics, Stanford University, Stanford, California 94305-4060

A. S. Schlachter, B. S. Rude, and R. J. McDonald
Accelerator and Fusion Research Division, Lawrence Berkeley Laboratory, University of California, Berkeley, California 94720
(Received 28 December 1987)

Electron-capture cross sections by 8.6-MeV/amu Ca^{18+}, Ca^{19+}, and Ca^{20+} beams were measured in gas targets from H_2 to Xe. Measurements were made of total electron capture as well as of electron capture in coincidence with projectile K x rays. Comparison with the eikonal approximation shows a reasonable agreement with the experimental data. The effect of various metastable states of the heliumlike Ca^{18+} ion created by electron capture for Ca^{19+} projectiles is analyzed, showing that these states play an important role in the detected x-ray yields.

I. INTRODUCTION

Electron-capture physics has been an object of intensive study during the past decade. Revealing features of this complex collision mechanism, such as the importance of the long-range character of the Coulomb interaction[1-3] or the use of target-centered continuum wave functions to mediate the capture reaction,[4,5] are currently coming to light and allowing a better understanding of the capture process. Despite this continuous effort, a unified treatment that accounts for a wide range of energies and collision symmetries has not yet come forth.

The present status of the theoretical development is limited to some specific situations such as symmetric collisions at low velocities in which a molecular picture can be used,[6] or asymmetric collisions at high velocities where a large number of investigations have been made in recent years.[1-5,7-16] At present, the search for a more comprehensive model is one of the main theoretical problems to be solved. In this regard, the study of the intermediate-velocity region (in which the projectile velocity approximately matches the Bohr velocity of the electron to be captured) is particularly important. As a matter of fact, it is in this regime that differences between various high-velocity theories emerge in a dramatic way even for asymmetric (weak perturbation) systems.

From the experimental point of view, many parameters (projectile and target species, charge state, energy) can and should be varied in order to make a selection among various theoretical models. So far, we have studied electron capture by intermediate-velocity, highly stripped ions with atomic numbers $Z_p = 6$, 54, and 92.[17-19] Electron-capture data for fast highly charged ions between $Z_p = 6$ and 54 are scarce.[16] The main purpose of this paper is to provide some systematic measurements in this Z_p region.

Beams of 345-MeV $Ca^{18+,19+,20+}$ were used to study single-electron capture on H_2, He, N_2, O_2, Ne, Ar, Kr, and Xe targets. The projectile velocity was such that $v_p = 0.93 Z_p$ (v_p is the projectile velocity in atomic units). In this way, we scanned collision systems ranging from $v_p \gg Z_t$ (Z_t is the target atomic number) to $v_p \ll Z_t$. Due to the wide range of v_p/Z_t, a full theoretical description of the experimental results is a difficult task. As a guide to interpret the experimental data, the eikonal approximation[14,17-19] was used throughout this work, even though it is applicable only if $v_p/(Z_t/n_t) \gg 1$, where n_t is the principal quantum number of the shell from which the target electron is captured.

The experimental method is described in Sec. II. Section III is separated into two subsections. The first presents the results of singles (noncoincidence) measurements which provide the total single-electron capture cross sections. The second presents the results of coincidence measurements in which only those electron capture events resulting in projectile K x-ray emissions are recorded. For a Ca^{19+} incident beam, the coincidence experiments revealed the importance of the metastable states of He-like Ca^{18+} in inhibiting the projectile K x rays detected. Finally, Sec. IV gives a summary of the main conclusions.

II. EXPERIMENT

The apparatus used in this experiment has been described in a previous paper[20] (paper II) and only a few details will be recalled. $Ca^{18+,19+,20+}$ beams from the Lawrence Berkeley Laboratory SuperHILAC were sent through a differentially pumped gas cell. The emerging beam was magnetically analyzed and directed into a detector box.

The detector box housed two kinds of detectors. For the singles measurements, a parallel-plate avalanche counter (PPAC) was used to record three charge states simultaneously. For the coincidence measurements, a pair of scintillation counters was used. Each scintillator was able to detect ions in two charge states. This was possible because one half of each scintillator was covered with a 1-μm-thick Al foil. Particles that hit that portion of the detector could be separated from the other group (with a different charge state) by the difference in pulse height produced in the scintillator.

For the coincidence measurements, a 16-mm-diam Si(Li) detector positioned at 90° with respect to the incident beam was used to detect the Ca x rays. The signals from the x-ray detector, together with those from the scintillators, were sent to fast-slow coincidence electronics and into a computer-based data acquisition system.

The data were analyzed by the growth-rate method from which the individual cross sections could be determined.[20] At least four pressures were measured for each charge-state yield and the background was frequently recorded to check contributions from the residual gas of the system (about 10^{-6} Torr). In the H_2 case, where the cross sections are particularly sensitive to the presence of impurities, care was exercised to keep the gas cell at low pressures for a long time before the gas was inserted. As a whole, uncertainties of 10% and 30% must, respectively, be assigned to the measured single and coincidence cross sections.

III. RESULTS AND DISCUSSION

A. Singles measurements

The measured total electron capture cross sections are presented in Table I and displayed in Fig. 1. In this figure, we also show the results of the coincidence measurements (which are discussed in Sec. III B) and the results of the eikonal calculations.[17,19] The solid, dashed-dotted, and dashed curves are the theoretical predications for Ca^{20+}, Ca^{19+}, and Ca^{18+} projectiles, respectively.

The eikonal calculations were carried out by using hydrogenic wave functions for projectile and target states. Inner and outer screening was taken into account, as described in Ref. 19. All the target electrons were included in the calculations and the summation over the projectile final states was extended up to $n=10$.

The prior form of the eikonal approximation was used in all cases. As shown below, for all targets used, capture is more likely to proceed into the higher projectile orbitals. Consequently, with few exceptions, Z_p/n_p is smaller than Z_t/n_t (n_p and n_t are the principal quantum numbers of the projectile and the target states, respectively). Hence the criterion described in Ref. 17 for use of the prior form is satisfied. Because the post-prior criterion greatly complicates the calculations and does not necessarily improve the results,[19] the prior form was also used for the lighter targets where the criterion for the prior form is not satisfied.

We used three molecular targets (H_2, N_2, and O_2). For these targets the projectile velocity is much larger than the electron orbital velocities. Under these conditions the capture cross sections are sensitive only to the higher-momentum components of the target wave functions and molecular effects are expected to be of minor importance. Thus we obtained the atomic cross sections for these targets by dividing the molecular cross sections by 2.

Figure 1 shows that the eikonal approximation reproduces the general trend of the experimental data. The difference between theory and experiment is about 50% for $v_p \approx 2Z_t$ and increases with Z_t, reaching a factor 3 for $v_p \approx Z_t/3$. A possible reason for the increase of the discrepancy with Z_t can be found with the aid of Fig. 2. In this figure we show the fractional contribution from the various target shells to the total capture cross section. It can be seen from this figure that for $Z_t > 15$ the contribution due to the L and M electrons becomes dominant. Hence we would expect the eikonal approximation to give improved results, since it requires $v_p \gg Z_t/n_t$, Z_p/n_p. However, the high-momentum components of these states are not properly described by the simple single-parameter wave function utilized. We expect that the use of a more refined set of target wave functions might improve the agreement with experiment.[19]

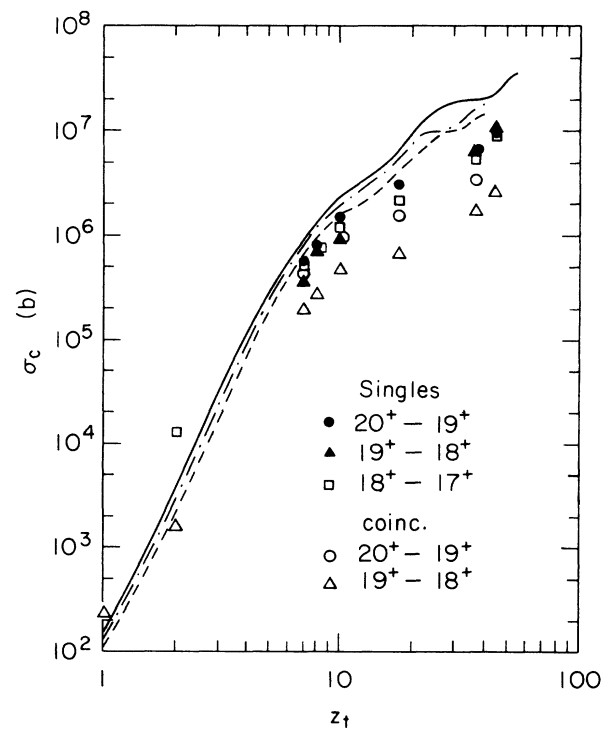The above discussion sets forth the importance of the

FIG. 1. Electron-capture cross sections by Ca^{20+}, Ca^{19+}, and Ca^{18+} beams for the singles measurements (●, ▲, and □) and for the coincidence measurements (○,△) as a function of the target atomic number Z_t. The theoretical curves are the eikonal calculations for Ca^{20+} (———), Ca^{19+} (—·—·—·), and Ca^{18+} (— — —). Some points are slightly shifted horizontally for better visualization.

TABLE I. One-electron-capture cross sections (singles measurements). (Typical uncertainties are ±10%.)

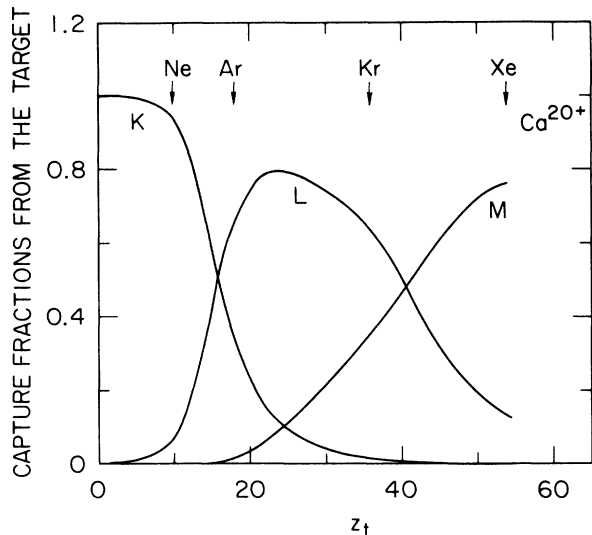| Target	Ca^{20+}	Ca^{19+}	Ca^{18+}
	(10^{-19} cm²/at.)		
H_2			0.13
He	5.8	3.7	5.3
N_2	8.4	7.3	7.8
Ne	15	9.1	12
Ar	32	22	22
Kr	62	62	53
Xe	94	110	88

FIG. 2. Calculated fractional electron capture from the various target shells into all the projectile states (up to $n = 10$) as a function of the target atomic number for Ca^{20+}.

higher target shells for the total electron capture. In fact, it can be seen from Fig. 2 that in the Ar case, for example, the fractional contribution from the L shell is about two times larger than the contribution from the K shell. But it is for the Ar K shell that velocity matching occurs $(Z_p \sim v_p \sim Z_{tK})$ and, as a consequence, we might have expected a larger contribution from the K shell than from the L shell. The reason for the inversion arises from the larger number of electrons in the L shell. Figure 3 shows the contribution per electron from each target shell to the
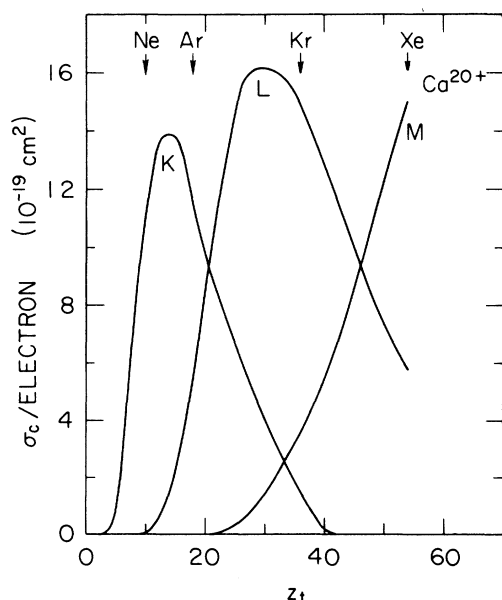
capture cross section. The summation over the projectile final states was done as before. Compared with Fig. 2, we can see that the maximum of L-shell contribution is clearly shifted towards a higher value of Z_t. For the Ar target, the K-shell contribution per electron is about two times larger than the contribution from the L shell, which is the result expected (at least qualitatively) from a velocity-matching argument. The results displayed in Fig. 2 can now be understood by realizing that there are four times more L than K electrons, yielding in this way a contribution of higher shells at a lower Z_t larger than expected. This discussion points out that the simple velocity-matching arguments commonly used to select the most important shell for a given projectile velocity must be used with care.

An interesting point that can be seen from Fig. 1 is that, for each target, the cross sections have a very weak charge-state dependence. This is true for both the experimental points as well and the theoretical predictions. This insensitivity of the cross sections to the projectile charge state, which we found also with $Z_p = 54$ and 92,[17,18] comes from the fact that in the present case, the capture preferentially occurs into the higher projectile orbitals. Hence the occupancy of the K-shell orbital by one or two electrons changes only the effective potential seen by an outer-shell electron and has only a small effect on the capture cross sections. Figure 4 shows the fractional contribution to the capture from the various projectile shells in Ca^{20+}. It is clear from this figure that the capture into the projectile K shell gives only a small contribution to the total cross section for the whole range of Z_t. As a consequence, approximately the same total capture cross section is obtained no matter whether the projectile K shell is empty or full. The predominance of the capture into the L shell compared to that into the K shell is basically due to the large number of final orbitals available in the L shell. Per orbital, almost the same cross section is obtained for these two shells, except for the lighter targets.

FIG. 3. Calculated electron capture *per electron* from the various target shells into all the projectile states (summed up to $n = 10$) as a function of the target atomic number for Ca^{20+}.
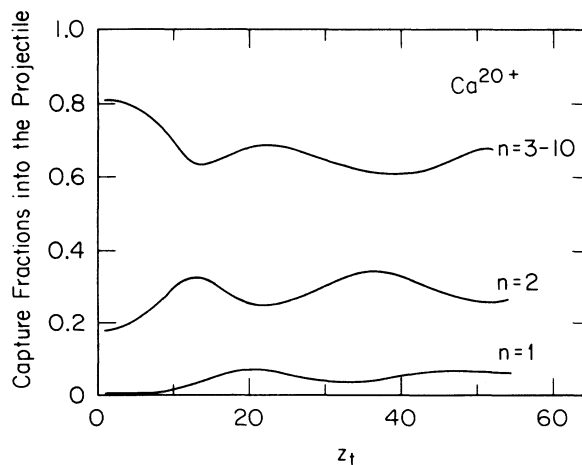

FIG. 4. Calculated fractional electron capture for all the target electrons into the specified projectile state as a function of the target atomic number for Ca^{20+}.

B. Coincidence measurements

The coincidence measurements were carried out by recording events where the emergent ion $Ca^{(q-1)+}$ (from an incident beam Ca^{q+}) are in coincidence with a projectile K x ray. In other words, the capture events in these measurements must take place into projectile states that provide, directly or by cascading, Ca K x rays emitted by the projectile in front of the detector window.

The experimental results for the Ca^{20+} and Ca^{19+} beams are presented in Table II, as well as in Fig. 1. The coincidence data were normalized by using the same normalization factor obtained from measurements of Ca^{19+} excitation cross sections.[20] It can be seen from Fig. 1 that the Ca^{20+} coincidence data lie only slightly below the singles data. The Ca^{19+} coincidence data, on the other hand, fall clearly below all the other data and are approximately a factor of 2 smaller than that of Ca^{20+} (Table II).

Our analysis of the singles data (Sec. III A) shows that the contribution from the $1s$ projectile state to the total capture cross section is small compared to that of projectile excited states. For this reason, we expect at first glance that the coincidence experiment should give results comparable to the singles measurements. However, the coincidence measurements have the further constraint that only those states which decay by K x-ray emission within the view of the detector are recorded. This restriction eliminates from the measurements some long-lived metastable states. As a consequence, the number of detected K x-ray–particle coincidence is reduced. We now make quantitative estimates of this reduction.

Let us consider the Ca^{20+} case. As a result of the capture into the L or higher shells, the L-shell states are filled following some kind of distribution. If we suppose, for simplicity, that this distribution is statistical, the $2s$ states contribute $\frac{1}{4}$ of these transitions. Under these conditions, only $\frac{3}{4}$ of the electrons captured into the L or higher shells are followed by a sufficiently fast x-ray emission. We then expect that the cross sections obtained in the coincidence measurements should be approximately $\frac{3}{4}$ of those obtained in the singles measurements. Naturally, this approximation neglects the contribution of the capture into the Ca^{20+} K shell, as well as those decaying modes that do not involve the projectile L shell (the $3p$-$1s$

transition, for example). In the present case, these contributions are not so large as to change significantly the scenario described above.

The Ca^{19+} case is more complicated. The resulting Ca^{18+} is a heliumlike ion in which some transitions involving the $n=2$ level have a very long lifetime due to restrictions imposed by angular momentum and parity conservation.[21] Figure 5 shows schematically the Ca^{18+} $n=1$ and 2 energy levels. Transitions which have the smallest lifetimes for decay into the $1s$ state are shown, as computed by Lin et al.[21] The subsequent analysis is based on these calculations.

Let us examine which transitions are able to contribute to the detected x-ray yield. The $2\,^3S_1$ $M1$ transition has a decay length (equal to $v_p\tau$, where τ is the half-life of the transition) of about 280 cm, much larger than the cell length (4.09 cm) and is disregarded. The two $E1$ transitions into the fundamental state have decay lengths of 2.5×10^{-5} cm and 8.4×10^{-5} cm and should be considered. The $2\,^3P_2-1\,^1S_0$ $M2$ transition has a calculated decay length of 5.4 cm, comparable to the cell length. Marrus and Schmieder[22] measured the lifetime of this transition in Ar^{16+}, finding a result that is about two times smaller than the calculation of Ref. 21. Since Ar is very close to Ca, it is possible that the calculated decay length (5.4 cm) is overestimated. The analysis of this transition becomes even more complicated since the $2\,^3P_2$ state can also decay into the long-lived $2\,^3S_1$ state by an $E1$ transition. According to Ref. 21, about 40% of the $2\,^3P_2$ transitions follow this decay mode which does not contribute to the measured x-ray yield.

As a first estimate, we assume that the $2\,^3P_2-1\,^1S_0$ branch is sufficiently short-lived to decay within the view of the detector, while the $2\,^3P_2-2\,^3S_1$ branch is not detected. Under these conditions, only about 60% of the population of the $2\,^3P_2$ state, together with the two fast $E1$ transitions, is detected. Assuming again a statistical population distribution over the various $n=2$ states, we infer that the measured coincidence cross sections for capture in Ca^{19+} should be about 2.6/8 of the singles cross sections.

In Fig. 6 we display the same theoretical eikonal total-capture calculations as in Fig. 1 together with the singles and corrected coincidence data. The coincidence data were multiplied by their respective decay factors estimated above in order to restore the total-capture data. The experimental points of the Ca^{20+} beam were multiplied

TABLE II. One-electron-capture cross sections (coincidence measurements). (Typical uncertainties are ±30%.) Numbers in square brackets are powers of ten.

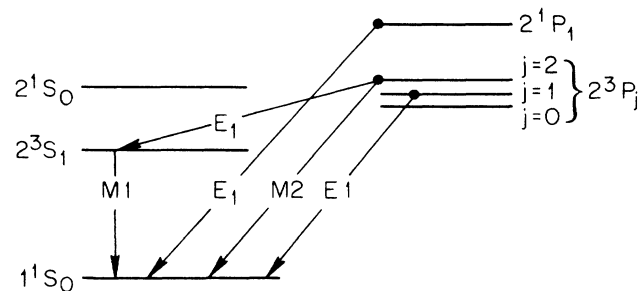| Target	$(10^{-19}$ cm^2/at.)	
	Ca^{20+}	Ca^{19+}
H_2		2.5[−3]
He		1.6[−2]
N_2	4.2	1.9
O_2		2.7
Ne	9.5	4.8
Ar	15	6.7
Kr	35	18
Xe		26

FIG. 5. Relevant energy levels and decay scheme of the heliumlike ion Ca^{18+}.
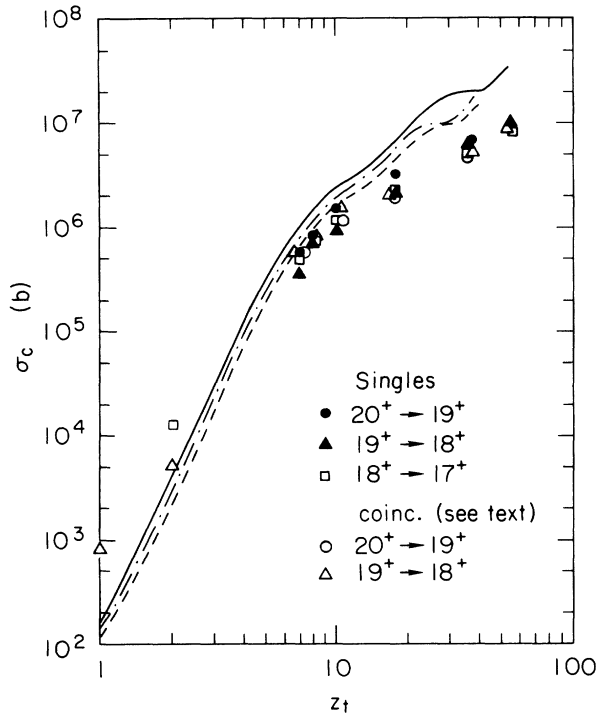
FIG. 6. Electron capture by Ca^{20+}, Ca^{19+}, and Ca^{18+} beams. The theoretical curves and the singles data are the same as in Fig. 1. The 20 + →19 + coincidence data were multiplied by $\frac{8}{6}$. The 19 + →18 + coincidence data were multiplied by 8/2.6 (see text.) Some points are slightly shifted horizontally for better visualization.

by $\frac{8}{6}$, whereas those from the Ca^{19+} were multiplied by 8/2.6. It is clear from this figure that all the experimental points now coalesce within experimental errors, corroborating the previous analysis and showing the consistency of the experimental data reported. (This coalescence also provides a check on the normalization of the coincidence data used in Ref. 20 and here.)

IV. CONCLUSIONS

In the present work, electron capture by highly ionized projectiles in several gaseous targets is studied. Our analysis is based on the eikonal approximation which gives a reasonable quantitative estimate of the experimental measurements and allowed to show the consistency of the data for all targets studied.

The projectile energy in this experiment was chosen to match approximately the projectile K-shell Bohr velocity. For the Ar target, this energy also matches its K-shell orbital velocity and this condition maximizes the capture

matrix element for K-shell capture. Despite this maximization, the contribution of higher-lying shells to the total capture cross sections is more important. In fact, in this intermediate-velocity regime, the L-shell contribution to the total electron capture is significant even if the projectile velocity is about three times larger than the orbital velocity of the L electron. The same applies to the M shell. The large influence of the outer shells prevents a good quantitative description of the experimental data if simple hydrogenic wave functions are used in the theory and may partially explain the failure of the eikonal approximation for the higher Z_t. It is interesting to note that the velocity matching condition favors an electron transfer that has an approximately symmetric matrix element $(v_p \approx Z_p \approx Z_t/n_t)$. It is then possible that a symmetrized version of the eikonal approximation[23,24] gives an improved description of the experimental data, even with hydrogenic wave functions. Further study of the total capture cross section in high-Z elements, using a symmetric eikonal approximation with hydrogenic wave functions and different basis sets, can elucidate the origin of the disagreement with the experimental data.

The coincidence measurements eliminate capture into the projectile K shell. We examined the important role played by metastable states, which hinder the detection of x rays originating from states with sufficiently long half-life. The analysis of the coincidence experiments becomes difficult if the decay length of the metastable state is comparable to the length of the target cell (or, to be more precise, to the length of the trajectory viewed by the x-ray detector which, in our case, is of the order of the cell length). Other sources of uncertainties are the accurate determination the detector solid angle and the type of distribution of captured electrons over the excited states, especially if the capture results in the formation of a two- or more-electron ion. Because of these factors, as well as experimental uncertainties, a precise determination of the contribution from these "medium"-lived states is not possible. For example, the contribution from the $2\,^3P_2 - 1\,^1S_0$ transition in Ca^{18+} could be reduced by as much as 50% without altering the analysis of the Ca^{19+} coincidence cross sections appreciably.

*On leave from Pontificia Universidade Catolica do Rio de Janeiro, Brazil.
†Permanent address: Department of Physics, Tsinghua University, Beijing, People's Republic of China.

‡Present address: Solid State Electronics Laboratory, Stanford University, Stanford, California 94305.
[1]D. P. Dewagen and J. Eichler, J. Phys B **18**, L65 (1985).
[2]D. P. Dewagen and J. Eichler, J. Phys. B **19**, 2939 (1986).

[3]D. P. Dewagen and J. Eichler, Nucl. Instrum. Methods B **23**, 160 (1987).

[4]J. Macek and S. Alston, Phys. Rev. A **26**, 250 (1982).

[5]S. Alston, Phys. Rev. A **27**, 2342 (1983).

[6]Wm. Lichten, Phys. Rev. **131**, A1025 (1965).

[7]P. J. Kramer, Phys. Rev. A **6**, 2125 (1972).

[8]J. S. Briggs, J. Phys. B **10**, 3075 (1977).

[9]Dž. Belkić, R. Gayet, and A. Salin, Phys. Rep. **56**, 279 (1979).

[10]J. Macek, J. Phys. B **18**, L71 (1985).

[11]J. H. McGuire, R. E. Kletke, and N. C. Sil, Phys. Rev. A **32**, 815 (1985).

[12]J. Eichler and F. T. Chan, Phys. Rev. A **20**, 104 (1979).

[13]F. T. Chan and J. Eichler, Phys. Rev. A **20**, 1841 (1979).

[14]J. Eichler, Phys. Rev. A **32**, 112 (1985).

[15]C. D. Lin, S. C. Suong, and N. L. Tunnel, Phys. Rev. A **17**, 1646 (1978).

[16]A. S. Schlachter, J. W. Stearns, K. H. Berkner, M. P. Stöckli, W. G. Graham, E. M. Bernstein, M. W. Clark, and J. A. Tanis, in *Abstracts of Contributed Papers, Fifteenth International Conference on the Physics of Electronic and Atomic Collisions, Brighton, 1987,* edited by J. Geddes, H. B. Gilbody, A.

A. Kingston, C. J. Latimer, and H. J. R. Walters (Queen's University, Belfast, 1987), p. 505.

[17]W. E. Meyerhof, R. Anholt, J. Eichler, H. Gould, Ch. Munger, J. Alonso, P. Thieberger, and H. E. Wegner, Phys. Rev. A **32**, 3302 (1985).

[18]R. Anholt, W. E. Meyerhof, X.-Y. Xu, H. Gould, B. Feinberg, R. J. McDonald, H. E. Wegner, and P. Thieberger, Phys. Rev. A **36**, 1586 (1987).

[19]R. Anholt, X.-Y. Xu, Ch. Stoller, J. Molitoris, W. E. Meyerhof, B. J. Rude, and R. J. McDonald, Phys. Rev. A **37**, 1105 (1988).

[20]X.-Y. Xu, E. C. Montenegro, R. Anholt, K. Danzmann, W. E. Meyerhof, A. S. Schlachter, B. Rude, and R. J. McDonald, preceding paper, Phys. Rev. A **38**, 1848 (1988).

[21]C. D. Lin, W. R. Johnson, and A. Dalgarno, Phys. Rev. A **15**, 154 (1977).

[22]R. Marrus and R. W. Schmieder, Phys. Rev. A **5**, 1160 (1972).

[23]J. M. Maidagan and R. D. Rivarola, J. Phys. B **17**, 2477 (1984).

[24]G. R. Deco, R. D. Piacentini, and R. D. Rivarola, J. Phys. B **19**, 3727 (1986).